

See discussions, stats, and author profiles for this publication at: <https://www.researchgate.net/publication/231644682>

Understanding Optical Activity in Single-Walled Carbon Nanotubes from First-Principles Studies

ARTICLE *in* THE JOURNAL OF PHYSICAL CHEMISTRY C · MAY 2010

Impact Factor: 4.77 · DOI: 10.1021/jp1011582

CITATIONS

18

READS

26

2 AUTHORS, INCLUDING:



Cecilia Noguez

Universidad Nacional Autónoma de México

87 PUBLICATIONS 2,569 CITATIONS

SEE PROFILE

Understanding Optical Activity in Single-Walled Carbon Nanotubes from First-Principles Studies

A. Sánchez-Castillo and Cecilia Noguez*

Instituto de Física, Universidad Nacional Autónoma de México, Apartado Postal 20-364, México D.F. 01000, México

Received: February 5, 2010; Revised Manuscript Received: March 24, 2010

The origin of optical activity in single-walled carbon nanotubes (SWNTs) is investigated by performing first-principles calculations of the circular dichroism (CD) spectrum. The calculated CD is in excellent agreement with experiments, which is understood in terms of the density of states and optical absorption, providing the nanotubes' absolute configuration. These results determine which nanotubes are present or not in CD measurements and their chirality, providing a framework to understand the enantioselectivity process in recent experiments. Additionally, these results offer theoretical support to understand chirality at the nanoscale and convey selectivity in synthesis, separation, and analysis using carbon nanotubes, which are important issues in molecular recognition, nanocatalysts, DNA assembly, as well as in biofunctionalization based on SWNT technology.

Introduction

Tremendous progress has been made toward the synthesis of monodisperse carbon single-walled nanotubes (SWNTs).¹ However, most of these methods result in SWNT mixtures that have a broad range of diameters, chiralities, and electronic properties, which are generally unsuitable for applications because their physical properties are not uniform. The separation and selection of SWNTs with desired properties is still a challenging task.^{1–6} SWNTs are chiral objects that resemble the wrapping of a graphene sheet to form a cylinder. The sheet can be rolled up in different ways, such that the lattice along the nanotube axis shows a helical twist, defining its chirality using the so-called chiral vector (n,m).⁷ Chiral nanotubes are, in practice, the most common ones in nature, and the two mirror-related forms of chiral SWNTs, right- (P) and left-handed (M), depend on which way the graphene sheet is rolled up.⁵ Important applications of chiral SWNTs in different fields ranging from materials science and molecular electronics to medicine and biochemistry are expected.⁸ For instance, it has been found that enriched P - or M -SWNTs are useful for sensing chiral molecules,⁹ studying novel effects induced by chirality in nanostructures,¹⁰ and understanding asymmetric catalysis.¹¹

Recently, scientists have turned their attention to sorting P - and M -SWNTs.^{2–6} In an effort to separate racemic mixtures, many mechanisms have been devised to obtain SWNTs with small diameters and well-defined helicities. Nowadays, the most successful approach that yields enantiomeric excess involves the wrapping of SWNTs with chiral molecules. These nanotubes were previously synthesized using a silica-supported Co–Mo catalyst (CoMo CAT).¹² Here, SWNTs are wrapped with chiral surfactants, such as DNA,² porphyrins,^{3–5} or sodium cholate,⁶ resulting in stable dispersed solutions. The selection of a nanotube with specific (n,m) indices seems to depend on the chiral agent or surfactant.^{4,5} On the other hand, the preference of a specific helicity, P over M or vice versa, seems to depend on which enantiomer, left- or right-handed, is used as surfactant.^{2–6} Both processes are sustained on the fact that enantiomers often do have different properties related to other

enantiomeric substances. Finally, physical techniques, such as ultrasonication and ultracentrifugation, are used to separate the desired SWNTs.¹

The success of the enantiomeric separation and/or enrichment was confirmed by measuring the electronic circular dichroism (CD) of the samples.^{2–6} This chiroptical technique detects slight differences in absorbance between left and right circularly polarized light and measures the optical activity of chiral substances. CD has been widely employed to characterize chiral molecules, surfaces, and solids. However, the experiments cannot unravel by themselves which enantiomer was successfully separated. To make progress in the field, comparison between experiments and a strong theoretical framework for a proper interpretation is crucial, which allows us to recognize and assign the absolute atomic configuration of the studied chiral objects.¹³ Although first-principles methodologies have been already implemented to perform calculations of CD spectra for relatively small molecules,^{14,15} this methodology has not been applied to explore the chiroptical properties of SWNTs. This is due to the huge computational effort involved and other methodological problems related with the gauge invariance treatment. An alternative approach to calculate CD spectra of nanoscale materials is to use DFT time-dependent perturbation theory.

In this paper, we study for the first time the origin of the optical activity in SWNTs by employing a recently developed time-dependent perturbation theory based on first-principles methods to calculate CD in nanostructures. The optical activity is explained in terms of the electronic density of states and optical absorption, which are inherent to each (n,m) SWNT. This study is useful for the identification and quantification of chirality in SWNTs, giving theoretical support to assign the absolute atomic configuration of enantiomer-enriched samples. The latter allows us to give further insight into recently reported experiments, where a very good agreement between theory and experiments is found. As a consequence, the present study will provide a strong theoretical support to understand fundamental phenomena related to molecular adsorption, functionalization, and enantioselectivity by using chiral SWNTs.

Computational Methods

We employ a density functional theory (DFT) formalism to perform structural optimizations, electronic structure

* To whom correspondence should be addressed. E-mail: cecilia@fisica.unam.mx.

calculations, and chiroptical property quantifications. Although significant progress was achieved during the past few years,^{16–18} it had not been possible to evaluate CD in SWNTs from first-principles calculations. Recently, a novel implementation based in a time-perturbed first-principles theory within DFT was developed.¹⁹ This method was adapted to exploit the versatility of the siesta package²⁰ to perform CD calculations for periodic and finite nanostructures composed of several hundred atoms. Here, SWNTs are modeled as infinite-length tubes constructed by periodically repeating a unit cell, which is defined by the indices (n, m) .⁷ We employ optimized atomic structures that are obtained as described elsewhere.¹⁸ The siesta package employs numerical atomic orbitals (2s and 2p for C) and a double- ζ polarized basis set. Troullier–Martin norm-conserving pseudopotentials²¹ and the Perdew and Zunger parametrization of the exchange–correlation potential within the local density approximation (LDA) were employed.²²

The macroscopic CD is given by the difference of the molar extinction between left and right circularly polarized light, which is related to the rotational strength as $\Delta\epsilon(\omega) = [(0.1343 \times 10^{-5})/(3300)]\beta(\omega)\tilde{\nu}^2$, where $\tilde{\nu}$ (cm^{-1}) is the wavenumber, and $\beta(\omega) = (-1/3\omega)\text{Tr}[\text{Re}(\tilde{G}_{\alpha\beta}(\omega))]$, which has units of a_0^3 , with a_0 as the Bohr radius (in atomic units), Re means the real part, and α and β label the respective Cartesian components.²³ The last expression was obtained from a time-dependent perturbation theory, where the Hamiltonian was expressed through an electromagnetic multipolar expansion of the vector and scalar potentials. Therefore, the CD spectrum is evaluated once the Rosenfeld equation of the rotational strength is calculated:²³

$$\tilde{G}_{\alpha\beta} = \frac{1}{\hbar} \sum_{j \neq n} \left(\frac{\langle n|\mu_\alpha|j\rangle\langle j|m_\beta|n\rangle}{\omega_{jn} - \omega} + \frac{\langle n|m_\beta|j\rangle\langle j|\mu_\alpha|n\rangle}{\omega_{jn} + \omega} \right) \quad (1)$$

Here the matrix elements $\langle n|\mu_\alpha|j\rangle$ and $\langle j|m_\beta|n\rangle$ correspond to the electric (μ) and magnetic (m) dipole moments, involving electron transitions from the ground state $|n\rangle$ with energy ϵ_n , to the excited state $|j\rangle$ with energy ϵ_j , such that ω is the frequency of the incident radiation field, which is circularly polarized, and $\hbar\omega_{jn} = \epsilon_j - \epsilon_n$. For more details see ref 19.

The magnetic moment depends on the origin of the unit cell due to the freedom in selecting the vector potential. This means that any arbitrary translation of the system can introduce a spurious effect on the CD. To overcome the origin dependence problem, we use the velocity representation for the calculation of the electric and magnetic dipole moments.¹⁹ Under periodic boundary conditions, it is better representing wave functions of the periodic system in terms of the momenta $\hat{\mathbf{p}}$ of the particles rather than positions. Therefore, making use of the commutation relation $[\mathbf{r}, \hat{H}] = (i\hbar/m)\hat{\mathbf{p}}$, where the magnetic momentum operator is $\hat{\mathbf{m}} = (q/2m)\mathbf{r} \times \hat{\mathbf{p}}$, we have

$$\tilde{G}_{\mu\mu}(\omega) = \frac{-q^2}{2m^3\hbar} \sum_{j \neq n, u} \frac{\gamma_{jn}}{\omega_{jn}} \times \left[\frac{P'_{\mu\mu}}{\omega_{uj}[(\omega_{jn} - \omega)^2 + \gamma_{jn}^2]} - \frac{P''_{\mu\mu}}{\omega_{nu}[(\omega_{jn} + \omega)^2 + \gamma_{jn}^2]} \right] \quad (2)$$

with

$$P'_{\mu\mu} = \langle n|p_\mu|j\rangle[\langle j|p_\nu|u\rangle\langle u|p_\nu|n\rangle - \langle j|p_\nu|u\rangle\langle u|p_\nu|n\rangle] \\ P''_{\mu\mu} = [\langle n|p_\nu|u\rangle\langle u|p_\nu|j\rangle - \langle n|p_\nu|u\rangle\langle u|p_\nu|j\rangle]\langle j|p_\mu|n\rangle$$

Furthermore, the linear momentum operator has an additional term due to the commutation of the nonlocal pseudopotentials and the position operator, which we have taken into account in the calculations.²⁴ This means that the hypervirial theorem is no longer valid and an extra phase has to be added in the magnetic susceptibility formulas,^{25,26} where only the first term is necessary to calculate the CD.²⁷ In some systems, this additional term is negligible, as it happens in the SWNTs studied here. To test the gauge invariance in our calculations, we did additional examinations by adding an arbitrary vector to the origin of the system and then calculating the CD spectra. We did not find changes in the CD spectra under arbitrary translations, concluding that our calculations are gauge invariance.

To calculate the electronic density of states (DOS), we perform integrations in the k -space over 50 points and use a grid of 150 k -points to calculate the optical absorption and CD spectra. Electronic transitions are computed over all occupied and unoccupied states generated by the extended-function basis set, where at least 50 empty bands are considered that guarantee convergence of the chiroptical properties. The simulated optical absorption and CD spectra have a 0.06 eV and 0.01 eV Gaussian broadening. DFT calculations are based on the single-particle Kohn–Sham equations. Therefore, many-body or excitonic effects are not implicitly included, and the electronic gap is underestimated. To overcome this, the electronic gap is opened with a constant energy shift that does not alter the electronic transitions; that is, the corresponding CD peaks, their width, intensity, and sign are not affected. This is known as the scissors operator. Since the origin of this gap underestimation is mainly due to many-body, excitonic, and local field effects,^{28,29} it is expected that this energy shift would be different for each SWNT and depends on their chirality and diameter. An additional factor that can alter the CD spectra is the solvent where nanotubes are dispersed.¹⁵ While many-body effects can be quantified using time-dependent DFT, excitonic and local field effects would require development of a different approach to explicitly compute them. Although some efforts have been done to include these effects, the numerical schemes are computationally demanding, such that it is not possible at this moment to include them in the calculation of CD for large nanotubes, as those reported in the experiments.

On the other hand, the DFT time-dependent perturbation theory employed here yields theoretical CD spectra in very good agreement with experiments, offering a good framework to understand the optical activity of SWNTs, as it is discussed below. For isolated small-diameter SWNTs, local field effects can be significant to explain depolarization effects that inhibit the optical absorption peaks occurring from the perpendicular polarization.²⁹ In contrast to this local optical response, the relevance of these effects in the CD spectra is unknown. Up to now, there is no theoretical or experimental evidence that local field or excitonic effects can or cannot play an important role in describing CD in SWNTs, but this possibility should be explored in the future. On the other hand, the very good agreement found in this work between theory and experiments suggests that these effects can be neglected in a first approximation.

Results and Discussion

Peng and co-workers^{3–5} achieved the enantiomeric enrichment of the (6,5) SWNTs by using chiral diporphyrins as surfactants;

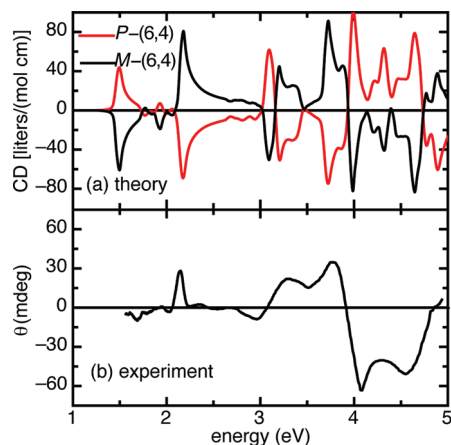


Figure 1. (a) Simulated CD of *P*- and *M*-(6,4). (b) Experimental data taken from ref 6.

that is, they separated (6,5) nanotubes with mostly one handedness. Mixtures with some enantiomeric excess but containing more than one kind of nanotubes, for instance, a mixture of (8,4) and (7,5) SWNTs along with others, were obtained. An alternative strategy was reported by Green and co-workers,⁶ who used chiral sodium cholate as surfactant to encapsulate SWNTs and exploited the small buoyant density variations to isolate the (6,4) SWNTs with enantiomeric excess. The same was done for the enantiomeric enrichment of (6,5) SWNTs. All of the samples were characterized by measuring the CD.^{3–6} Therefore, we study the CD spectra of the (6,4), (6,5), and (8,4) SWNTs, which were recently employed by different experimental groups. In the experiments, the SWNTs are well-dispersed in the solution, therefore, we have assumed that they do not interact with each other and are randomly oriented. Thus, we directly compare the computed angular average CD of one nanotube with the corresponding experimental curve for the (6,4) and (6,5) nanotubes. For the (8,4) SWNT, it is not possible to compare directly with experiments because CD was measured in a nonenriched sample, that is, a mixture of nanotubes with different concentrations and unknown enantiomeric excess for each one. In this case, the CD spectrum is a combination of the CD signals corresponding to each nanotube and depends on the concentration, enantiomeric excess, and handedness of the nanotubes present in the sample.

In Figure 1a are shown the calculated CD spectra of the right-handed nanotube *P*-(6,4) and its mirror image *M*-(6,4). The enantiomers show identical optical activity, except that they are opposite in sign. This fact makes difficult the assignment of the SWNT handedness, especially if there is not theoretical support. In Figure 1b, we show the measured CD of a sample containing one enriched enantiomer of the (6,4) SWNT taken from ref 6. The measured CD shows a well-defined line shape with three positive and four negative peaks, whose energies are listed in Table 1. The calculated CD was blue-shifted 0.4 eV. According to our calculations, the measured CD corresponds to the *M* enantiomer of (6,4), in agreement with the experimental assumption.⁶ We find that the calculated CD is in very good agreement with the experimental curve. The small differences in width and intensity can be attributed to different factors, for instance, the enantiomeric excess, isomeric purity, temperature, solvation effects, and solvent–solute interactions,¹⁵ as well to local field or excitonic effects, not included in the calculations.

CD peaks arise in the optical absorption bands given by the electron transitions in the vicinity of the van Hove (VH) singularities, which are typical of quasi-one-dimensional sys-

TABLE 1: Energies (in eV) of VH Transitions and CD Peaks

(6,4) SWNT (energies are blue-shifted 0.4 eV)				
VH transition	energy value	absorption energy	CD peaks exp ref 6	CD peaks, this work
E_{11}	1.54	1.57		1.57
E_{21}	2.00	1.98	2.03	1.99
E_{22}	2.22	2.23	2.14	2.26
E_{32}	3.20	3.10	2.96–3.28	2.99–3.20
E_{33}	3.73	3.77	3.75	3.77
E_{34}	4.30	3.92	4.09–4.56	4.09–4.56
(8,4) SWNT (energies are blue-shifted 0.3 eV)				
exp ref 4				
E_{11}	1.13	1.17		1.13
E_{12}	1.69	1.66		
E_{21}	1.57	1.57		1.54
E_{22}	2.14	2.09	2.10	2.10
E_{33}	2.99	3.08	3.23	3.04
E_{43}	3.42	3.40		3.43
(6,5) SWNT (energies are blue-shifted 0.3 eV)				
exp refs 4 and 6				
E_{11}	1.22	1.26	1.27, –	1.29
E_{12}	1.76	1.74	1.87–2.13, 1.79–2.04	1.53–1.91
E_{22}	2.06	2.19	2.21, 2.19	2.25
E_{32}	2.80	2.88	2.54–3.31, 2.55–3.19	2.63–3.16
E_{33}	3.26	3.40	3.64, 3.61	3.44
E_{44}	4.13	4.02	–, 4.11	4.02

tems, like SWNTs. Different kinds of interband transitions $\mu \rightarrow \mu'$ with energy $E_{\mu\mu'} \equiv E_{\mu'} - E_{\mu}$ are allowed. Here, μ and μ' label the occupied and empty bands, respectively, which result from periodically repeating the unit cell to form the SWNT. In this quasi-one-dimensional system with VH singularities, the following selection rules apply. Electronic transitions parallel to the nanotube axis are induced with $\mu = \mu'$ only, while for the perpendicular direction, only electronic transitions with $\mu' = \mu \pm 1$ are allowed. Thus, to understand the origin of the CD peaks, we have calculated the DOS of the (6,4) nanotube, as well as its optical absorption arising from parallel and perpendicular electron transitions. In Figure 2a, DOS is shown and the energies $E_{\mu\mu'}$ of the allowed parallel electron transitions are indicated. In Table 1, the energies $E_{\mu\mu'}$ in the first column correspond to the values at which the maxima of the DOS bands are located. In the second column of Table 1, the energies are related to the corresponding parallel and perpendicular optical absorption peaks in Figure 2b,f. These peaks are associated with the main features of the CD spectrum in Figure 2d, which is decomposed into its parallel (zz) and perpendicular ($1/2(xx + yy)$) components with respect to the nanotube's axis, given by the corresponding terms of the trace of the G tensor in eq 2.¹⁹ These components are shown in Figure 2c,e, respectively.

Total CD spectrum of *M*-(6,4) shows alternate positive and negative peaks, whose magnitude increases as the energy does, in agreement with experiments.^{3–6} For parallel transitions, the E_{11} , E_{22} , and E_{33} electron transitions give rise to absorption signals, which are associated with CD peaks at 1.57, 2.26, and 3.77 eV, respectively. The first peak was not reported in the experiment,⁶ probably due to the low resolution of the experimental setup at such energy. However, a similar peak was measured at about 1.65 eV, as observed in Figure 1b. Perpendicular transitions, E_{21} , E_{32} , and E_{34} , also play an important role, particularly at higher energies. For instance, it is found from calculations that E_{21} at 1.98 eV slightly modifies the CD line

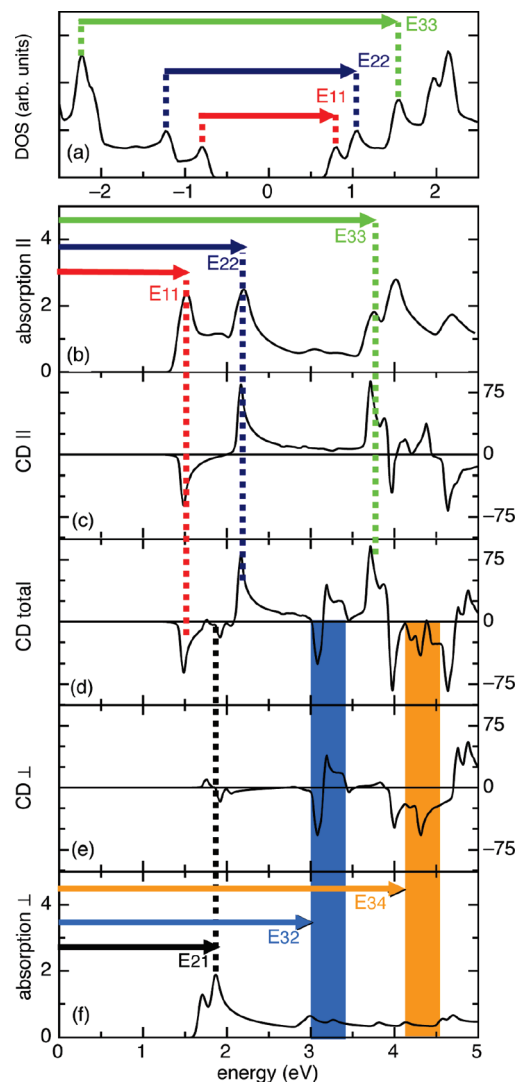


Figure 2. (a) DOS, (b) parallel (||), and (f) perpendicular (\perp) optical absorption, (c) || and (e) \perp components of (d) the total CD of M -(6,4). CD is given in $\text{L mol}^{-1} \text{cm}^{-1}$, and the optical absorption in terms of the imaginary part of the nanotube's polarizability. The blue and orange bands indicate where the Cotton effects arise.

shape, while Cotton effects³⁰ are observed around E_{32} and E_{34} at 3.10 and 3.92 eV, respectively. The blue and orange bands in Figure 2d–f indicate where the Cotton effects arise. Transition E_{32} gives rise to the small negative–positive structure observed in the experiment.⁶ On the other hand, transition E_{34} originates the large negative structure that can be seen from 4 to 4.5 eV. In the experiment, the latter was assigned to E_{44} ; however, this transition takes place at larger energies, as can be deduced from DOS. Comparing these results to experiments in ref 6, we find the same sign sequence of the seven peaks (–, +, –, +, +, –, –), where the first two are related to E_{21} and E_{22} , respectively, the next two with E_{32} due to Cotton effects, the fifth one with E_{33} , and the last two arise from E_{34} also due to Cotton effects.

Figure 3a shows the simulated CD for P - and M -(8,4). In Figure 3b, the measured CD obtained for a nonenriched sample that contains a mixture of different SWNTs is shown, including the (8,4). We find that parallel transitions E_{11} , E_{22} , and E_{33} are responsible for the CD peaks at 1.13, 2.10, and 3.04 eV, respectively. The perpendicular transition E_{21} at 1.54 eV slightly modifies the line shape of CD, while E_{43} gives rise to the negative peak at 3.43 eV. In the experiment, two peaks were

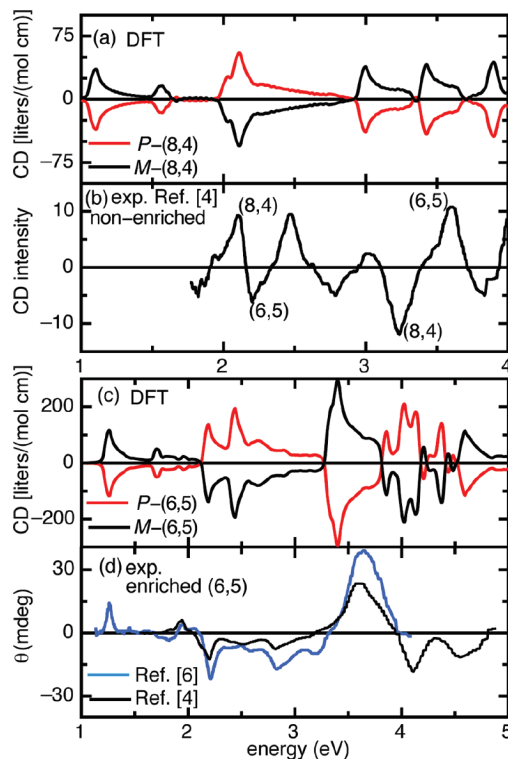


Figure 3. (a) Simulated CD of P - and M -(8,4). (b) Experimental data taken from ref 4 (arbitrary units). (c) Simulated CD of P - and M -(6,5). (d) Experimental data taken from refs 4 and 6. Both calculated CDs are blue-shifted 0.3 eV.

assigned to (8,4) corresponding to E_{22} and E_{33} .^{3,4} As shown in Table 1, the experimental and calculated energies for the E_{22} peak are the same, but there is a difference of 0.2 eV for the peak corresponding to E_{33} . This discrepancy can be attributed to different factors, for example, the peak could belong to another SWNT present in the experimental sample, or the peak can be shifted due to many-body and excitonic effects.³¹

In Figure 3c,d, the calculated and two different measurements of CD spectra for (6,5) are shown, respectively. The experimental spectra show some differences among them, which can be attributed to the different experimental conditions, for instance, the solvent.^{4,6} The measured CD corresponds to the M enantiomer of (6,5), in disagreement with the experimental assumption.⁶ In this case, we find that parallel transitions E_{11} , E_{22} , E_{33} , and E_{44} are responsible for the CD peaks at 1.29, 2.25, 3.44, and 4.02 eV, respectively. The perpendicular transition E_{21} from 1.53 to 1.91 eV slightly modifies the line shape of CD, while E_{32} gives rise to the negative structure from 2.63 to 3.16 eV. As shown in Table 1, the experimental and calculated energies for E_{11} and E_{22} peaks are in very good agreement, but there is a difference of 0.2 eV for the peak corresponding to E_{33} . The overall agreement of theory with enriched experiments is excellent. On the other hand, the CD average of (6,5) and (8,4) SWNTs does not resemble the experimental CD in Figure 3b, indicating that there are more SWNTs in the mixture that contribute to that measurement. The present theoretical results imply that the sign of the E_{22} CD peak for the left-handed species (6,4) and (6,5) is opposite. The same is also true for M -(8,4). This finding would invalidate the assumption proposed in ref 6 that all chiral SWNTs having a positive E_{22} transition in the CD peak can be identified as left-handed (M), while those with a negative peak are right-handed (P).

Conclusions

The optical activity of SWNTs has been studied in terms of their chiral indices, electronic density of states, and optical absorption. On the basis of the calculated circular dichroism, the origin of the optical activity and the absolute atomic configuration or handedness of the (6,4), (8,4), and (6,5) SWNTs are found. These results are compared with available experiments, where a very good agreement is found and the absolute configuration of the nanotubes is assigned. At low energies, it is established that the main peaks arise from electron transitions induced by light polarized along the nanotube's axis, while perpendicular transitions do not cause additional peaks but can slightly modify the spectra line shape. At larger energies, perpendicular transitions are responsible for the CD peaks. These results provide a strong theoretical support to understand chirality at the nanoscale for fundamental and applied problems that involve the synthesis, characterization, and functionalization of SWNTs, which are important in electronics, biology, medicine, and pharmacology, among other disciplines.

Acknowledgment. Financial support from UNAM (PAPIIT IN106408) and CONACyT (48521) is acknowledged. We thank DGSCA-UNAM Supercomputer Center for valuable computer resources used in this research.

References and Notes

- (1) Hersam, M. *Nat. Nanotechnol.* **2008**, *3*, 387, and references therein.
- (2) Dukovic, G.; Balaz, M.; Doak, P.; Berova, N. D.; Zheng, M.; Mclean, R. S.; Brus, L. E. *J. Am. Chem. Soc.* **2006**, *128*, 9004.
- (3) Peng, X.; Komatsu, N.; Bhattacharya, S.; Shimawaki, T.; Aonuma, S.; Kimura, T.; Osuka, A. *Nat. Nanotechnol.* **2007**, *2*, 361.
- (4) Peng, X.; Komatsu, N.; Kimura, T.; Osuka, A. *J. Am. Chem. Soc.* **2007**, *129*, 15947.
- (5) Peng, X.; Komatsu, N.; Osuka, A. *ACS Nano* **2008**, *2*, 2045.
- (6) Green, A.; Duch, M.; Hersam, M. *Nano Res.* **2009**, *2*, 69.
- (7) Saito, R.; Dresselhaus, G.; Dresselhaus, M. S. *Physical Properties of Carbon Nanotubes*; Imperial College Press: London, U.K., 1998.
- (8) Conyers, J. L.; Moore, V. C.; Lackey, M.; Partha, R.; Cherukuri, P.; Hudson, J. L.; Leonard, A.; Tour, J. M.; Huff, J. *Nanomed.: Nanotechnol., Biol. Med.* **2006**, *2*, 304.
- (9) Vardanega, D.; Picaud, F.; Girardet, C. *J. Chem. Phys.* **2007**, *127*, 194702.
- (10) Smith, D. K. *Chem. Soc. Rev.* **2009**, *38*, 684.
- (11) Xing, L.; Xie, J.-H.; Chen, Y.-S.; Wang, L.-X.; Zhou, Q.-L. *Adv. Synth. Catal.* **2008**, *350*, 1013–1016.
- (12) Bachilo, S. M.; Balzano, L.; Herrera, J. E.; Pompeo, F.; Resasco, D. E.; Weisman, R. B. *J. Am. Chem. Soc.* **2003**, *125*, 11186–11187.
- (13) Berova, N.; Nakanishi, K.; Woody, R. W. *Circular Dichroism, Principles and Applications*, 2nd ed.; Wiley-VCH: New York, 2000.
- (14) Autschbach, J.; Ziegler, T.; van Gisbergen, S. J. A.; Baerends, E. J. *J. Chem. Phys.* **2002**, *116*, 6930–6940.
- (15) Crawford, T. D.; Tam, M. C.; Abrams, M. L. *J. Phys. Chem. A* **2007**, *111*, 12057.
- (16) Tasaki, S.; Maekawa, K.; Yamabe, T. *Phys. Rev. B* **1998**, *57*, 9301.
- (17) Samsonidze, G. G.; Grneis, A.; Saito, R.; Jorio, A.; Filho, A. G. S.; Dresselhaus, G.; Dresselhaus, M. S. *Phys. Rev. B* **2004**, *69*, 205402.
- (18) Sanchez-Castillo, A.; Roman-Velazquez, C. E.; Noguez, C. *Phys. Rev. B* **2006**, *73*, 045401.
- (19) Hidalgo, F.; Sanchez-Castillo, A.; Noguez, C. *Phys. Rev. B* **2009**, *79*, 075438.
- (20) Soler, J. M.; Artacho, E.; Gale, J. D.; Garcia, A.; Junquera, J.; Ordejon, P.; Sanchez-Portal, D. *J. Phys.: Condens. Matter* **2002**, *14*, 2745.
- (21) Troullier, N.; Martins, J. L. *Phys. Rev. B* **1991**, *43*, 1993.
- (22) Perdew, J. P.; Zunger, A. *Phys. Rev. B* **1981**, *23*, 5048.
- (23) Barron, L. *Molecular Light Scattering and Optical Activity*, 2nd ed.; Cambridge University Press: Cambridge, U.K., 2004.
- (24) Starace, A. F. *Phys. Rev. A* **1971**, *3*, 1242–1245.
- (25) Ismail-Beigi, S.; Chang, E. K.; Louie, S. G. *Phys. Rev. Lett.* **2001**, *87*, 087402.
- (26) Pickard, C. J.; Mauri, F. *Phys. Rev. Lett.* **2003**, *91*, 196401.
- (27) Varsano, D.; Espinosa-Leal, L. A.; Andrade, X.; Marques, M. A. L.; di Felice, R.; Rubio, A. *Phys. Chem. Chem. Phys.* **2009**, *11*, 4481.
- (28) Spataru, C. D.; Ismail-Beigi, S.; Benedict, L. X.; Louie, S. G. *Phys. Rev. Lett.* **2004**, *92*, 077402.
- (29) Marinopoulos, A. G.; Reining, L.; Rubio, A.; Vast, N. *Phys. Rev. Lett.* **2003**, *91*, 046402.
- (30) The Cotton effect is the characteristic change in CD in the vicinity of an absorption band of a substance. In a wavelength region where the light is absorbed, the absolute magnitude of CD at first varies rapidly with wavelength, crosses zero at absorption maxima, and then again varies rapidly with wavelength but in opposite direction.^{13,23}
- (31) Korovyanko, O. J.; Sheng, C.-X.; Vardeny, Z. V.; Dalton, A. B.; Baughman, R. H. *Phys. Rev. Lett.* **2004**, *92*, 017403.

JP1011582